Eur. Phys. J. D **18**, 37–49 (2002)
DOI: 10.1140/e10053-002-0004-9

THE EUROPEAN PHYSICAL JOURNAL D
EDP Sciences

Molecular flow and wall collision age distributions

C. Baumgarten[1], B. Braun[1,2], G. Court[3], G. Ciullo[4], P. Ferretti[4], G. Graw[1], W. Haeberli[5], M. Henoch[2], R. Hertenberger[1], N. Koch[2], H. Kolster[1,6,a], P. Lenisa[4], A. Nass[2], S.P. Pod'yachev[2,7], D. Reggiani[4], K. Rith[2], M.C. Simani[8], E. Steffens[2,b], J. Stewart[3,9], and T. Wise[5]

[1] Sektion Physik, Ludwigs-Maximilians-Universität München, 85748 Garching, Germany
[2] Physikalisches Institut, Universität Erlangen-Nürnberg, 91058 Erlangen, Germany
[3] Physics Department, University of Liverpool, Liverpool L69 7ZE, UK
[4] Istituto Nazionale di Fisica Nucleare and Universita', 44100 Ferrara, Italy
[5] Department of Physics, University of Wisconsin-Madison, Madison, Wisconsin 53706, USA
[6] Nationaal Instituut voor Kernfysica en Hoge-Energiefysica (NIKHEF), 1009 DB Amsterdam, The Netherlands
[7] Institute of Automation and Electrometry of SB RAS, Russia
[8] Department of Physics and Astronomy, Vrije Universiteit, 1081 Amsterdam, The Netherlands
[9] DESY Zeuthen, 15738 Zeuthen, Germany

Received 9 July 2001 and Received in final form 18 September 2001

Abstract. The use of storage cells has become a standard technique for internal gas targets in conjunction with high energy storage rings. In case of spin-polarized hydrogen and deuterium gas targets the interaction of the injected atoms with the walls of the storage cell can lead to depolarization and recombination. Thus the number of wall collisions of the atoms in the target gas is important for modeling the processes of spin relaxation and recombination. It is shown in this article that the diffusion process of rarefied gases in long tubes or storage cells can be described with the help of the one-dimensional diffusion equation. Mathematical methods are presented that allow one to calculate collision age distributions (CAD) and their moments analytically. These methods provide a better understanding of the different aspects of diffusion than Monte Carlo calculations. Additionally it is shown that measurements of the atomic density or polarization of a gas sample taken from the center of the tube allow one to determine the possible range of the corresponding density weighted average values along the tube. The calculations are applied to the storage cell geometry of the HERMES internal polarized hydrogen and deuterium gas target.

PACS. 47.45.Dt Free molecular flows – 51.20.+d Viscosity, diffusion, and thermal conductivity – 29.25.Pj Polarized and other targets

1 Introduction

Several recent experiments [1,2], including the HERMES experiment [3–5], which are performed at high or medium energy lepton or hadron storage rings, make use of internal nuclear polarized gas targets. These targets have the advantage of high purity and the possibility of fast spin reversal. The relatively low target thickness allows experimenters the use of gas targets in storage rings with reasonable lifetimes of the stored beam. Often storage cells are used which are open-ended long tubes mounted so that the beam of the storage ring passes along their axis [6–8]. Figure 1 shows the HERMES target storage cell as an example [9]. A side tube attached to the storage cell center is used for the injection of the beam of nuclear polarized atoms that are produced by an atomic beam source (ABS) [10,11]. The injected atoms collide with the walls of the storage cell and diffuse into the storage ring beam pipe where they are removed by a high capacity pumping system. Inside the storage cell the gas density exhibits a triangular profile along the beam path of the storage ring. The diffusing atoms can intercept the path of the stored beam several times, thereby increasing the achievable target thickness by about two orders of magnitude compared to a free jet target. This technique allows for the production of a usable target thickness of up to $10^{14}\,\mathrm{nucl\,cm^{-2}}$ using nuclear spin-polarized atomic hydrogen or deuterium. This corresponds to gas densities of about 10^{12} to $10^{13}\,\mathrm{atoms\,cm^{-3}}$ and the behavior of the gas can be described by molecular flow, *e.g.* atom-atom collisions in the volume can be neglected.

[a] *Current address*: Laboratory for Nuclear Science, Massachusetts Institute of Technology, Cambridge, Massachusetts 02139, USA.
[b] e-mail: steffens@physik.uni-erlangen.de

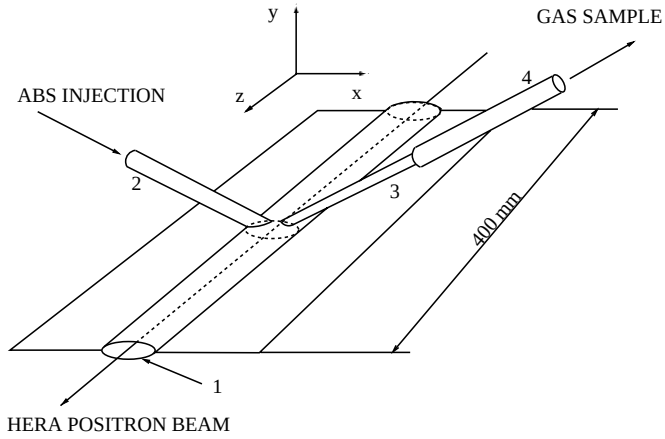

Fig. 1. Geometry of the HERMES storage cell used from 1996 until 1999. 1: Beam tube (BT) elliptically shaped 9.8 by 29 mm, $2\,L = 400\,\mathrm{mm}$ long. 2: Injection tube (IT), 10 mm diameter, 100 mm long. 3: Sampling tube (ST), 5 mm diameter, 100 mm long. 4: Extension tube (ET), 10 mm diameter, 120 mm long. The angle between injection and sample tubes and the horizontal plane is 30°. A storage cell with a smaller beam tube cross-section was installed in December 1999.

It is further assumed that the atoms or molecules are physically adsorbed by the surface for a short time period. During this time the atoms are in thermal equilibrium with the surface, sticking there or hopping from site to site until they evaporate back into the gas phase. As adsorption and desorption are decoupled, the desorption can be assumed to be isotropic and therefore is described by a $\cos\theta$-distribution with θ being the desorption angle relative to the surface normal. If spin-polarized atoms are used as target gas, wall collisions will induce spin depolarization and recombination of these atoms, which will reduce the polarization of the target.

In this article we discuss the interplay of the above mentioned effects with the diffusion of atoms inside the storage cell. Since both recombination and wall depolarization can be treated in an analogous way, only the case of recombination is discussed in the following. The reader is referred to reference [12] for a complete treatment of the case of wall depolarization.

The distribution $n(b, z)$ of atoms with collision age b along the longitudinal coordinate z inside the storage cell will be derived and compared with the distributions obtained by a molecular flow simulation [12–16]. Expressions for the *atomic* density in the presence of recombination are calculated. It will be shown that in the case of weak recombination (depolarization) it is sufficient to know the average number of wall collisions $\bar{b}(z)$ of the particles at position z in order to determine the atomic density (polarization).

In case of the HERMES target a sample of the target gas leaves the center of the storage cell and is analyzed by a Breit-Rabi polarimeter (BRP) [12,13,17,18], which measures the polarization of the atoms, and a target gas analyzer [12,14,15], which measures the ratio of atoms to molecules. The average properties along the length of the target cell are computed based on the extracted sample. As the atoms can either recombine or depolarize as they diffuse out of the target cell, the calculation of the average atomic fraction and average polarization over the target cell requires a detailed understanding of the gas transport processes inside the target cell.

If wall relaxation and recombination are assumed to be uniform all over the inner surface of the storage cell, the properties of the target gas can be calculated analytically as a function of the measured values [12,14,19]. However, this scenario does not seem to be realistic since there have been indications for non-uniform changes of the surface properties during operation of the HERMES target in the 27.5 GeV HERA electron ring with beam currents of up to 50 mA [12,15]. Hence it is necessary to investigate all possible distributions of atomic density and polarization for any kind of non-uniform surfaces which are compatible with the measured properties of the sample beam. The problem of the calculation of average properties of a gas in a storage cell, when only the properties of a gas sample from the cell center are measured, is called the *central sampling problem*. An exact solution of the central sampling problem is in general not possible, because a measurement of the central value does not contain enough information. Nevertheless, one is able to determine limits for the possible range of the average gas properties, if the corresponding properties in the storage cell center are known. These limits are sufficiently narrow under the operating conditions of the HERMES target to allow for the determination of the target properties with small errors.

2 The diffusion approximation

2.1 Molecular flow and diffusion

Gas diffusion in the low pressure regime is called *molecular flow* and has first been investigated by Knudsen [20], Smoluchowski [21] and Gaede [22].

According to Fick's First Law the gas flow Φ along the axis of a long tube is proportional to the gradient of the density n (or pressure, since $p = nkT$)

$$\Phi = -DS\frac{\partial p}{\partial z}, \tag{1}$$

where S is the cross-section of the tube and D the diffusion constant [23]. For tubes of arbitrary cross-section D is approximately given by

$$D = \frac{4}{3}\frac{S}{U}\,\bar{v}, \tag{2}$$

where U is the circumference of the tube and $\bar{v}$ is the mean velocity of the atoms. Using equation (1) it can be shown that D is related to the *conductance* C of the tube by $C = DS/L$ where L is the length of the tube. Later it has been shown that equation (2) has to be corrected for tubes of finite length [24–28]. If R is the radius of the tube,

equation (2) is exact only in the limiting case $R/L \to 0$. Equation (1) can also be written as

$$j = -D\,\frac{\partial n}{\partial z}, \tag{3}$$

where n is the particle density and j the particle flow density. The continuity equation can be expressed by

$$\frac{\partial n}{\partial t} + \frac{\partial j}{\partial z} = q, \tag{4}$$

where the source density q can be used to describe the (non-diffusive) appearance of atoms, which are injected *ballistically* by an ABS into the storage cell center, or their disappearance by chemical reactions like recombination ($H_1 + H_1 \to H_2$). If the gradient of the diffusion constant D vanishes, which is true for tubes of constant cross-section and temperature, equations (3, 4) can be combined to the *diffusion equation*

$$\frac{\partial n}{\partial t} = D\,\frac{\partial^2 n}{\partial z^2} + q. \tag{5}$$

Spin-polarized gas is steadily injected into the HERMES storage cell center through the injection tube by an atomic beam source (ABS) [9]. This process can be modeled by a steady delta-like source at $z = 0$. It follows that the density is constant in time ($\partial n/\partial t = 0$) and equation (5) becomes

$$D\frac{\mathrm{d}^2 n}{\mathrm{d}z^2} = -\frac{\dot{n}_{\mathrm{inj}}}{S}\,\delta(z), \tag{6}$$

where the constant $\dot{n}_{\mathrm{inj}}$ represents the number of injected atoms per unit time. If one uses the approximation of vanishing density at the end, a solution of equation (6), that fulfills the boundary condition $n(L) = 0$, is a triangular density profile

$$\begin{aligned} n(z) &= n_0\,(1 - \frac{|z|}{L}) \quad \text{for } |z| < L \\ n(z) &= 0 \qquad\qquad\quad \text{for } |z| > L, \end{aligned} \tag{7}$$

where $2\,L$ is the length of the complete tube, $n_0 = n(0) = \dot{n}_{\mathrm{inj}}\,/C$ is the central density and C is the conductance seen by the injected atomic beam, which in case of the HERMES storage cell (see Fig. 1) is given by the sum of the conductances of both halves of the beam tube C_{BT}, the injection tube C_{IT} and the reciprocal sum of the conductances of sample- and extension-tube C_{ST} and C_{ET}:

$$C = 2\,C_{\mathrm{BT}} + C_{\mathrm{IT}} + \frac{C_{\mathrm{ST}}\,C_{\mathrm{ET}}}{C_{\mathrm{ST}} + C_{\mathrm{ET}}}\,. \tag{8}$$

In the following, if not explicitly included, the side tubes are neglected.

The mean collision age $\bar{b}(L)$ at the end of a long tube is given by [19]

$$\bar{b}(L) = \frac{3}{32}\,\left(\frac{UL}{S}\right)^2. \tag{9}$$

The average time τ_{d} that the atom has spent inside the storage cell is [19]

$$\tau_{\mathrm{d}} = \frac{3}{8}\,\frac{L^2 U}{S\bar{v}}\,. \tag{10}$$

The average time of flight τ_{f} between two wall collisions is

$$\tau_{\mathrm{f}} = \frac{\tau_{\mathrm{d}}}{\bar{b}} = \frac{4}{\bar{v}}\frac{S}{U}\,. \tag{11}$$

Consider a burst of atoms injected at position $z = 0$ and time $t = 0$. The distribution of the atoms at time $t > 0$ is described by the solution of equation (5) with $q = 0$. If the description of the diffusion process is restricted to a single tube with a single value of τ_{f} or to a combination of tubes with the same value of τ_{f}, the time since the injection of the burst can be expressed by the collision age b of the atoms using $t = \tau_{\mathrm{f}} b$. Steady injection is understood as a continuous stream of bursts injected into the cell, where the injection at position $z = 0$ is treated as a boundary condition. Hence equation (5) can be written as

$$\frac{\partial n}{\partial b} = \frac{\partial n}{\partial t}\tau_{\mathrm{f}} = D\tau_{\mathrm{f}}\frac{\partial^2 n}{\partial z^2} = \tilde{D}\,\frac{\partial^2 n}{\partial z^2}, \tag{12}$$

with a modified diffusion constant $\tilde{D} = D\tau_{\mathrm{f}} = (16/3)S^2/U^2$. Since recombination and spin relaxation processes are predominantly caused by wall collisions, it is necessary to investigate where and how often the atoms hit the wall. One way to obtain this information is a molecular flow simulation [29]. But it will be shown that the solution of equation (12) also provides this information in reasonable approximation.

2.2 Solution of the diffusion equation

Using the method of separation of variables one finds that

$$n(z,b) = \frac{n_0}{\bar{b}}\sum_{k=0}^{\infty}\exp\left(-\frac{\pi^2}{8}(2k+1)^2\frac{b}{\bar{b}}\right)\cos\left(\frac{(2k+1)\pi z}{2L}\right) \tag{13}$$

with $\bar{b} = \bar{b}(L)$ given by equation (9) is a solution of equation (12). It fulfills the boundary condition $n(\pm L, b) = 0$. Equation (13) is a Fourier series expansion and converges rapidly for high collision ages $b > \bar{b}/2$. For low collision ages ($b < \bar{b}/2$) one may instead use [15]

$$n(z,b) = \frac{n_0}{L}\sqrt{\frac{\tilde{D}}{\pi\,b}}\sum_{k=-\infty}^{\infty}(-)^k\exp\left(-\frac{(z-2\,k\,L)^2}{4\tilde{D}b}\right). \tag{14}$$

According to Sommerfeld both solutions are related by the transformation relation of ϑ-functions [30]. They describe the distribution of atoms or molecules as functions of position z and collision age b with the boundary condition of vanishing density at the end of the tube and for

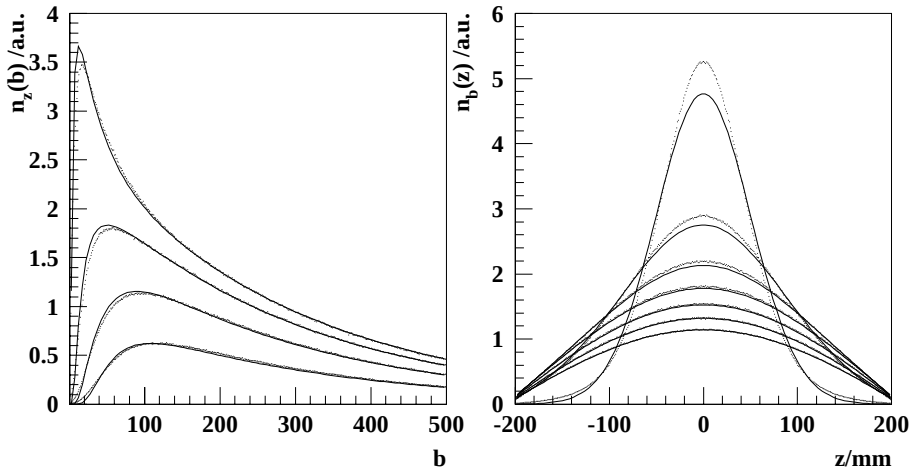

Fig. 2. Comparison of calculated (lines) and simulated (dots) density distributions $n(b, z)$ for an elliptical storage cell of $29.8 \times 9.8\,\mathrm{mm}^2$ diameter and $2L = 400\,\mathrm{mm}$ length in arbitrary units. Left: $n_z(b)$ for positions $z = 40, 80, 120$ and $160\,\mathrm{mm}$ (top to bottom). Right: $n_b(z)$ for collision ages $b = 20, 60, 100, 140, 180, 220$ and 260 (top to bottom). The non-vanishing density at the ends ($z = \pm L$) was taken into account by an artificial increase of the length L in equation (13) by 8 mm. The calculation made use of the first 100 terms of the sum in equation (13).

a storage cell without side tubes. In reality the density at $|z| = L$ does not vanish. One may take this into account by an artificial increase of the length L in equation (13) by about the radius R of the tube. Figure 2 compares the result of equation (13) with the result of a molecular flow simulation [29] for an elliptical tube of $29.8 \times 9.8\,\mathrm{mm}^2$ diameter of length $2\,L = 400\,\mathrm{mm}$. While the agreement is only approximate for low collision ages, it improves with increasing b. For $b > \bar{b}/2$ the difference is less than 2%.

2.3 Collision age distribution and recombination

In this section the atomic density in the presence of recombination will be calculated from the collision age distribution. Furthermore a simple approximation for the case of weak recombination will be derived.

A *collision age distribution* (CAD) $N_{\mathrm{CAD}}(z, b)$ describes the probability to find an atom with collision age b at position z, *i.e.* in the interval $[z \ldots z + \mathrm{d}z]$. It is given by the normalized solution $n(z, b)$

$$N_{\mathrm{CAD}}(z, b) = \frac{n(z, b)}{\int_0^\infty n(z, b)\mathrm{d}b}\,. \tag{15}$$

The denominator corresponds to a triangular shaped density distribution, which reaches n_0 at $z = 0$ and vanishes at $z = \pm L$. The Fourier series expansion of the triangular shaped density distribution is obtained by integrating equation (13)

$$n(z) = \int_0^\infty n(z, b)\mathrm{d}b = n_0 \sum_{k=0}^{\infty} \frac{8}{\pi^2} \frac{\cos\left(\frac{\pi(2k+1)z}{2L}\right)}{(2k+1)^2}\,. \tag{16}$$

By definition (equation (15)) the distribution $N_{\mathrm{CAD}}(z, b)$ is normalized to unity

$$\int_0^\infty N_{\mathrm{CAD}}(z, b)\,\mathrm{d}b = 1. \tag{17}$$

Let γ_{r} be the recombination probability per wall collision. It has been shown that in case of the HERMES target the dominant recombination mechanism is the reaction of a atom from the gas phase with an atom chemically bond to the surface. This process is independent of the target gas density since the coverage of the chemically bond sites can assumed to be close to unity [12]. If γ_{r} is additionally independent on position the probability ρ_a for an atom to survive b wall collisions is

$$\rho_a(b) = (1 - \gamma_{\mathrm{r}})^b \simeq \mathrm{e}^{-\gamma_{\mathrm{r}} b}, \tag{18}$$

where the approximation holds for $\gamma_{\mathrm{r}} \ll 1$ and $b \gg 1$. For polarized targets γ_{r} is typically of the order $10^{-2} \ldots 10^{-5}$. Thus the approximation is justified. The average probability $\rho_a(z, \gamma_{\mathrm{r}})$ that the atoms in $[z \ldots z + \mathrm{d}z]$ inside the target cell did not recombine, is given by the survival probability $\rho_a(b)$ for a given collision age b times the probability of collision age b summed over all possible collision ages

$$\begin{aligned}\rho_a(z, \gamma_{\mathrm{r}}) &= \sum_{b=0}^{\infty} N_{\mathrm{CAD}}(z, b)\,\rho_a(b) \\ &\simeq \int_0^\infty N_{\mathrm{CAD}}(z, b)\,\exp\left(-\gamma_{\mathrm{r}} b\right)\,\mathrm{d}b.\end{aligned} \tag{19}$$

Equation (19) corresponds to a Laplace-transformation. The Taylor series of $\rho_a(z, \gamma_{\mathrm{r}})$ in γ_{r} can be expressed by

the *moments* $\beta_m(z) = \langle\, b^m \,\rangle\,(z)$ of $N_{\mathrm{CAD}}(z,b)$, defined by

$$\beta_m(z) = \int_0^\infty b^m N_{\mathrm{CAD}}(z,b)\,\mathrm{d}b. \tag{20}$$

Hence one obtains

$$\begin{aligned}\rho_a(z,\gamma_\mathrm{r}) &= \sum_{m=0}^{\infty} \left.\frac{\partial^m \rho_a(z,\gamma_\mathrm{r})}{\partial \gamma_\mathrm{r}^m}\right|_{\gamma_\mathrm{r}=0} \frac{\gamma_\mathrm{r}^m}{m!} \\ &= 1 - \beta_1(z)\gamma_\mathrm{r} + \frac{1}{2}\beta_2(z)\gamma_\mathrm{r}^2 - \ldots\end{aligned} \tag{21}$$

If γ_r is small, $\rho_a(z,\gamma_\mathrm{r})$ can be approximated to the nth order if the first n moments of the CAD are known. If on the other hand $\rho_a(z,\gamma_\mathrm{r})$ is known, the moments $\beta_m(z)$ can be derived using equation (19)

$$\beta_m(z) = (-)^m \left.\frac{\mathrm{d}\rho_a(z,\gamma_\mathrm{r})}{\mathrm{d}\gamma_\mathrm{r}}\right|_{\gamma_\mathrm{r}=0}. \tag{22}$$

A straight forward way to approximate $\rho_a(z,\gamma_\mathrm{r})$ to the nth order is to skip terms of higher order in γ_r on the right side of equation (21). This method of approximation becomes meaningless for high values of γ_r. In first order approximation $\rho_a(z,\gamma_\mathrm{r})$ for instance becomes negative for $\beta_1\gamma_\mathrm{r} > 1$. This problem can be avoided using an approximation $\tilde{N}_{\mathrm{CAD}}(b)$ of the collision age distribution (Eq. (13))

$$N_{\mathrm{CAD}}(b,z) \simeq \tilde{N}_{\mathrm{CAD}}(b,z) = \frac{1}{\bar{b}}\,\exp\left(-\frac{b}{\bar{b}(z)}\right). \tag{23}$$

Equation (19) then yields

$$\rho_a(\gamma_\mathrm{r},z) = \frac{1}{1+\bar{b}(z)\gamma_\mathrm{r}}, \tag{24}$$

where $\bar{b}(z)$ corresponds the average collision age at position z and is therefore identical to the first moment β_1. A generalization for higher order approximations is then given by

$$\rho_a(\gamma_\mathrm{r},z) = \frac{1}{1+\beta_1(z)\,\gamma_\mathrm{r} + (\beta_1^2(z) - \frac{1}{2}\beta_2(z))\,\gamma_\mathrm{r}^2 + \ldots}, \tag{25}$$

where the coefficients in the denominator are given by the formulae for the inversion of series [31] applied to equation (21). In the next section the exact solution for $\rho_a(\gamma_\mathrm{r},z)$ for a long tube and constant γ_r will be derived.

2.4 Calculation of atomic density and moments from collision age distributions

The atomic density for a given number of wall bounces $n_a(z,b)$ in the presence of uniform recombination can be computed by multiplying the density distribution in the absence of recombination, derived in equation (13), with the survival probability $\rho_a(b)$

$$\begin{aligned}n_a(z,b) &= n(z,b)\,\rho_a(b) \\ &= \frac{n_0}{\bar{b}} \sum_{k=0}^{\infty} \exp\left(-\frac{\pi^2}{8}(2k+1)^2\frac{b}{\bar{b}} - \gamma_\mathrm{r}\,b\right) \\ &\quad \times \cos\left(\frac{(2k+1)\pi z}{2L}\right).\end{aligned} \tag{26}$$

The total atomic density $n_a(z,\gamma_\mathrm{r})$ is obtained by integration over all collision ages

$$n_a(z,\gamma_\mathrm{r}) = \int_0^\infty n_a(z,b)\mathrm{d}b = n_0 \sum_{k=0}^{\infty} \frac{8}{\pi^2} \frac{\cos\left(\frac{\pi(2k+1)z}{2L}\right)}{(2k+1)^2 + \frac{8}{\pi^2}\bar{b}\gamma_\mathrm{r}}. \tag{27}$$

As a consequence of the multiplication with the factor $\exp(-\gamma_\mathrm{r}\,b)$ in equation (26), $n_a(z,b)$ is no longer a solution of equation (12). In the presence of recombination, the atomic density $n_a(z,b)$ is reduced by the number of atoms recombining with the bth wall collision at position z which is $\gamma_\mathrm{r} n_a(z,b)$. Hence $\gamma_\mathrm{r} n_a(z,b)$ has to be subtracted from the right side of equation (12) and one obtains

$$\frac{\partial n_a(z,b)}{\partial b} = \tilde{D}\,\frac{\partial^2 n_a(z,b)}{\partial z^2} - \gamma_\mathrm{r} n_a(z,b). \tag{28}$$

The above given differential equation is solved by equation (26). Integrating equation (28) over all collision ages yields the following ordinary differential equation:

$$n_a(z,\infty) - n_a(z,0) = 0 = \tilde{D}\frac{\mathrm{d}^2 n_a(z)}{\mathrm{d}z^2} - \gamma_\mathrm{r}\,n_a(z), \tag{29}$$

where it was used that $n_a(z,b)$ vanishes for both zero and infinite collision age b. The solution of equation (29), which fulfills the boundary condition $n(L) = 0$, is

$$n_a(z,\gamma_\mathrm{r}) = n_a(0)\,\frac{\sinh\left(\sqrt{x}\,y\right)}{\sinh\left(\sqrt{x}\right)}, \tag{30}$$

where x and y are defined by $x = (L^2/\tilde{D})\gamma_\mathrm{r}$ and $y = (L-|z|)/L$. Equation (30) is identical to equation (27), which is a Fourier series expansion of the sinh-function.

If the atomic density in the center of the cell is known, equation (30) describes the atomic density profile inside the target cell including effects of uniform recombination. In the case of the HERMES target, the atomic flux into the storage cell center is constant and hence the atomic density $n_a(0)$ decreases with increasing recombination. Equation (30) can therefore not be applied directly. If one integrates equation (6) over an infinitesimal interval around $z = 0$, one obtains

$$\left.\frac{\mathrm{d}n_a}{\mathrm{d}z}\right|_{z\to+0} - \left.\frac{\mathrm{d}n_a}{\mathrm{d}z}\right|_{z\to-0} = -\frac{\dot{n}_{\mathrm{inj}}}{C_{\mathrm{BT}}\,L}, \tag{31}$$

where the side tubes are neglected. Since the integration was carried out around an arbitrarily small interval, the

integrated surface area is negligible and the relation holds in the presence of recombination. Since the tube is symmetric both gradients on the left of equation (31) are the same and thus

$$\dot{n}^{\mathrm{inj}} = -2\, C_{\mathrm{BT}}\, L \left.\frac{\partial n_a}{\partial z}\right|_{z\to+0} . \tag{32}$$

With equation (30)

$$n_a(0) = \frac{\dot{n}^{\mathrm{inj}}}{2\, C_{\mathrm{BT}}} \frac{\tanh\sqrt{x}}{\sqrt{x}} . \tag{33}$$

It is useful to define the *effective* conductance C^{eff} for atoms at the entrance of a tube given by

$$C^{\mathrm{eff}} = \frac{\dot{n}^{\mathrm{inj}}}{n_a(0) - n_a(L)} = \frac{\dot{n}_{\mathrm{inj}}}{n_a(0)} = C_{\mathrm{BT}} \frac{\sqrt{x}}{\tanh\sqrt{x}} . \tag{34}$$

C^{eff} accounts for the loss in center density of atoms from recombination in the cell and $C^{\mathrm{eff}} > C_{\mathrm{BT}}$ holds for $\gamma_{\mathrm{r}} > 0$. The expression for C^{eff} can be used to simplify the relation between the central atomic density $n_a(0)$ and the injected flux $\dot{n}_{\mathrm{inj}}$, given by equation (33)

$$n_a(0) = \frac{\dot{n}_{\mathrm{inj}}}{2\, C^{\mathrm{eff}}} . \tag{35}$$

Equations (33, 35) may now be applied to equation (30) to yield the atomic density in the storage cell with the boundary condition of a constant flux of injected atoms

$$n_a(z,\gamma_{\mathrm{r}}) = \frac{\dot{n}_{\mathrm{inj}}}{2\, C_{\mathrm{BT}}} \frac{\sinh\left(\sqrt{x}\, y(z)\right)}{\sqrt{x}\cosh\left(\sqrt{x}\right)} . \tag{36}$$

Equation (36) still neglects the injection and sample tube and can therefore not be applied directly to the HERMES storage cell. The analytical solution for a storage cell in Figure 1 is given in [12].

The probability that an atom at position z has survived recombination is equal to the ratio of the atomic densities with and without recombination

$$\rho_a(z,\gamma_{\mathrm{r}}) = \frac{n(z,\gamma_{\mathrm{r}})}{n(z,\gamma_{\mathrm{r}})|_{\gamma_{\mathrm{r}}=0}} . \tag{37}$$

ρ_a can be calculated analytically using $n_a(z,\gamma_{\mathrm{r}})$ given by equation (36)

$$\rho_a(x,y) = \frac{\sinh\left(\sqrt{x}y\right)}{\sqrt{x}y\cosh\left(\sqrt{x}\right)} . \tag{38}$$

The z dependence of equation (38) for various values of γ_{r} is shown as solid lines in Figure 3.

If one expands the hyperbolic functions in numerator and denominator of equation (38) into Taylor series of their arguments and uses the formula for division of series in the variable x [31], $\rho_a(z,\gamma_{\mathrm{r}})$ can be written in the following way

$$\rho_a(x,y) = \left[1 + \frac{y^2-3}{6}x + \frac{y^4 - 10\,y^2 + 25}{120}x^2 + \ldots\right], \tag{39}$$

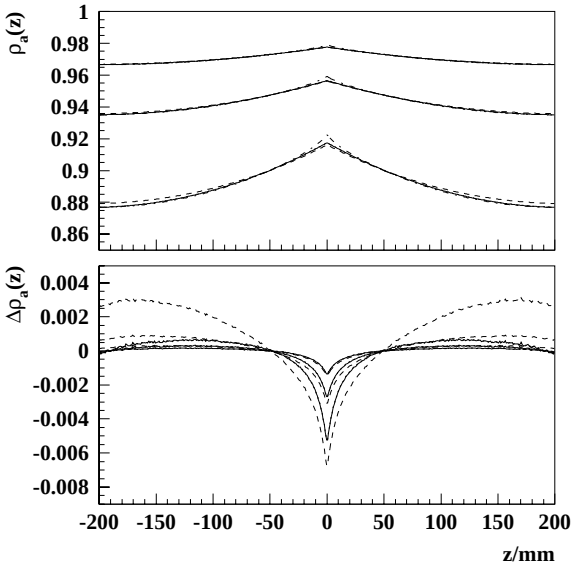

Fig. 3. Upper figure: survival probability $\rho_a(z)$ in a storage cell *vs.* position z. The solid lines are calculated using equation (38). The first order approximation [Eq. (24)] is shown by dashed lines and the second order approximation [Eq. (25)] by the dotted lines (hidden by solid line). For these two cases β_1 and β_2 were calculated from equation (40). The results shown by the dash-dotted lines were obtained using equation (19) with $N_{\mathrm{CAD}}(z,b)$ from a molecular flow simulation. All curves were calculated assuming a uniform recombination probability γ_{r} (top to bottom) of $\gamma_{\mathrm{r}} = 10^{-4}, 2\times10^{-4}$ and 4×10^{-4}. Lower figure: relative difference $\Delta\rho_a(z,\gamma_{\mathrm{r}})$ between equation (38) (solid lines), equation (24) (dashed lines) and equation (25) (dotted lines, hidden by solid lines) and the result of the Monte Carlo simulation for the same conditions.

which corresponds to a Taylor series in x. It was shown in equation (22) that the coefficients of the Taylor series expansion of ρ_a are related to the moments of the CAD. By comparison of equations (39, 22) the following moments of the CAD are obtained:

$$\begin{aligned}\beta_1(z) &= \bar{b} = \frac{\varepsilon^2}{6}(3-y^2)\\ \beta_2(z) &= \frac{\varepsilon^4}{60}(25 - 10\,y^2 + y^4) = \frac{\varepsilon^4}{60}(5-y^2)^2\\ &\ldots,\end{aligned} \tag{40}$$

where $\varepsilon = L/\sqrt{\tilde{D}}$ and $y = 1-|z|/L$. The average collision age at the end of the tube ($y = 0$) is in agreement with equation (9)

$$\bar{b}(L) = \frac{\varepsilon^2}{2} = \frac{3}{32}\left(\frac{UL}{S}\right)^2 . \tag{41}$$

The density weighted average collision age $\bar{\beta}_1$ is given by

$$\begin{aligned}\bar{\beta}_1 &= 2\int_0^1 \beta_1(y)\, y\, \mathrm{d}y = \frac{5}{12}\,\varepsilon^2 = \frac{5}{4}\beta_1(z=0)\\ &= \frac{5}{6}\,\beta_1(z=L) = \beta_1(z = \frac{\sqrt{2}-1}{\sqrt{2}}L).\end{aligned} \tag{42}$$

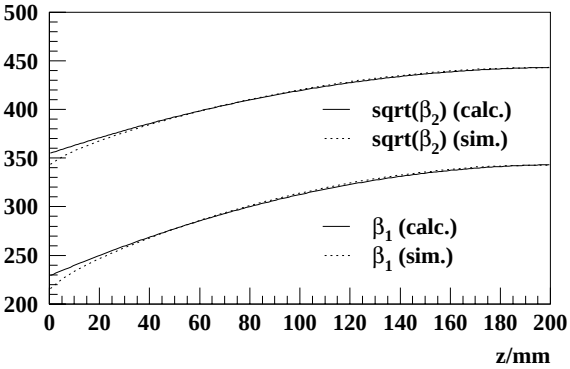

Fig. 4. Moments β_1 and β_2 of the CAD of an elliptically shaped tube like the HERMES beam tube vs position z. The solid lines are calculated using equation (40), the dotted curves are obtained by a molecular flow simulation. The length L was increased in the calculation by 8 mm in order to take the finite conductance at the end of the cell into account. The second moment is shown as $\sqrt{\beta_2}$. For both moments the agreement is rather good except for the very center.

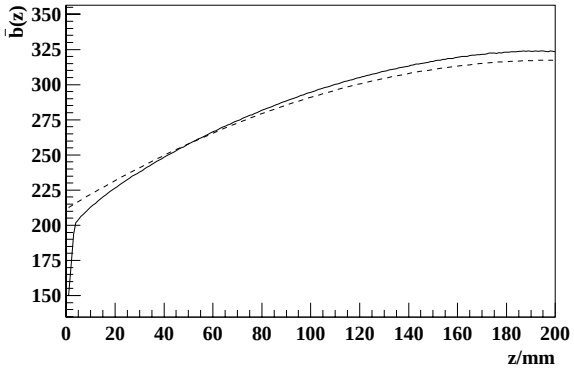

Fig. 5. Average collision age $\bar{b}(z)$ in the beam tube of the HERMES storage cell obtained by a molecular flow simulation including all side tubes (solid line) and by equation (45) (dashed line). The drop of $\bar{b}(z)$ in the storage cell center is caused by the injected jet. Besides this jet, the difference between calculation and simulation is $\leq 4\%$.

Figure 4 shows a comparison of the calculations with the results of a molecular flow simulation. Figure 3 shows a comparison of the different methods to obtain the average survival probability $\rho_a(z,\gamma_\mathrm{r})$. The different methods agree well in the case of weak recombination, which is the situation of interest in polarized gas targets.

The relative difference $\Delta\rho_a^\mathrm{mc}(z,\gamma_\mathrm{r})$ of the result obtained by equation (19) with $N_\mathrm{CAD}(b,z)$ from a Monte Carlo simulation of molecular flow and the first order analytical solution $\rho_a^{(1)}(z,\gamma_\mathrm{r})$ (Eq. (24) with $\bar{b}(z) = \beta_1(z)$ using Eq. (40)) for $L = 208\,\mathrm{mm}$

$$\Delta\rho_a(z,\gamma_\mathrm{r}) = \left|\frac{\rho_a^{(1)}(z,\gamma_\mathrm{r}) - \rho_a^\mathrm{mc}(z,\gamma_\mathrm{r})}{\rho_a^\mathrm{mc}(z,\gamma_\mathrm{r})}\right|, \qquad (43)$$

is shown in the lower plot of Figure 3 for $\gamma_\mathrm{r} \leq 4\times10^{-4}$ or ρ_a above 0.88. The curves show, that the atomic density decreases with increasing recombination, the effect is smaller in the center and increases with increasing $|z|$. The figure clearly illustrates that a measurement of the atomic density at $z = 0$ has to be corrected in order to obtain the *average* atomic density. The magnitude of the correction increases with increasing $|z|$ and increasing γ_r. It will be shown later, that in case of the HERMES target, the difference $\Delta\rho_a(z)$ resulting from different methods of calculation can be neglected compared to the systematic uncertainty introduced when γ_r is allowed to vary along the cell.

The above calculations are accurate for a simple tube with a source in the center. At the HERMES storage cell (Fig. 1) two additional tubes are connected in the center, one for the injection of atoms, and one for sampling of atoms with the polarimeter and gas analyzer, respectively. Equations (40) are only accurate if the total conductance of all side tubes C_side can be neglected compared to the total conductance of the cell: $C_\mathrm{side} \ll C_\mathrm{cell}$. This is not the case for the HERMES storage cell. But since the atomic density $n(z,\gamma_\mathrm{r})$ can also be calculated in the presence of side tubes [12,14], one can determine the average collision age using the derivatives of $\rho_a(\gamma_\mathrm{r}) = n(z,\gamma_\mathrm{r})/n(z,0)$. If additional tubes of constant cross-section are connected in the center of the storage cell, the atomic density along the jth tube is given by

$$n^{(j)}(z,\gamma_\mathrm{r}) = \frac{\dot{n}^\mathrm{inj}}{\sum_i C_i^\mathrm{eff}}\,\frac{\sinh\sqrt{x_j}\,y_j}{\sinh\sqrt{x_j}}, \qquad (44)$$

where C_i^eff are the individual conductances (x_i and ε_i, defined correspondingly) and $y_j = 1-|z|/L_j$ is a function of the coordinate along the axis of the jth tube. The average collision age $\bar{b}_j(z)$ in the jth tube is given by

$$\bar{b}_j(z) = \frac{1}{3}\,\frac{\sum_i C_i\,\varepsilon_i^2}{\sum_i C_i} + \frac{\varepsilon_j^2}{6}(1-y_j^2). \qquad (45)$$

It is worth mentioning that the absolute value of $\bar{b}$ depends on the side tubes, while the first derivative along z does not. Figure 5 shows a comparison of equation (45) with the result of a molecular flow simulation.

2.5 Homogeneous beam tube

If one applies equation (44) to the HERMES storage cell and assumes uniform recombination inside the beam tube ($\gamma_\mathrm{r}^\mathrm{BT} = const = \gamma_\mathrm{r}$) and negligible recombination inside the side tubes ($\gamma_\mathrm{r}^\mathrm{IT} = \gamma_\mathrm{r}^\mathrm{ST} = \gamma_\mathrm{r}^\mathrm{ET} \simeq 0$, for the symbols see Fig. 1), one obtains the following expression for the central density:

$$n^{(j)}(0,\gamma_\mathrm{r}) = \frac{\dot{n}^\mathrm{inj}}{\sum_i C_i^\mathrm{eff}}, \qquad (46)$$

so that using equation (37), $\rho_a(0)$ is given by:

$$\rho_a(0) = \frac{\sum_i C_i}{\sum_i C_i^\mathrm{eff}} \qquad (47)$$
$$= \frac{C_\mathrm{IT} + C_\mathrm{ETST} + 2\,C_\mathrm{BT}}{C_\mathrm{IT} + C_\mathrm{ETST} + 2\,C_\mathrm{BT}\varepsilon^\mathrm{BT}\sqrt{\gamma_\mathrm{r}}/\tanh\left(\varepsilon^\mathrm{BT}\sqrt{\gamma_\mathrm{r}}\right)},$$

where C_{ETST} is the combined conductance of sample and extension tube ($1/C_{\mathrm{ETST}} = 1/C_{\mathrm{ET}} + 1/C_{\mathrm{ST}}$). The density weighted average value $\bar{\rho}_a$ is given by

$$\bar{\rho}_a = \frac{\int_{-L}^{L} n^{\mathrm{BT}}(z,\gamma_{\mathrm{r}})\,\mathrm{d}z}{\int_{-L}^{L} n^{\mathrm{BT}}(z,0)\,\mathrm{d}z} = \frac{1}{L n^{\mathrm{BT}}(0,0)} \int_{-L}^{L} n^{\mathrm{BT}}(z,\gamma_{\mathrm{r}})\,\mathrm{d}z. \tag{48}$$

The calculation yields

$$\bar{\rho}_a = \rho_a(0)\,\frac{2\,\sinh\left(\varepsilon\sqrt{\gamma_{\mathrm{r}}}\right)}{\varepsilon\sqrt{\gamma_{\mathrm{r}}}\left[1+\cosh\left(\varepsilon\sqrt{\gamma_{\mathrm{r}}}\right)\right]}\,. \tag{49}$$

This formula may be used in situations where uniform and density independent recombination can be assumed. A uniform surface is not a realistic assumption in case of the HERMES target cell. In the next sections non-uniform situations will therefore be discussed.

2.6 Differential collision ages

If the recombination probability depends on the position z along the cell, information is required on how many collisions the atoms of the sampled gas performed within the interval $z \ldots z + \mathrm{d}z$ – called the *differential collision age*.

One assumes a storage cell without recombination in side tubes $\gamma_{\mathrm{r}}^{\mathrm{IT}} = \gamma_{\mathrm{r}}^{\mathrm{ST}} = \gamma_{\mathrm{r}}^{\mathrm{ET}} = 0$ and a beam tube that is split into an inner region $|z| < L_0$, where $\gamma_{\mathrm{r}}^{\mathrm{BT}} = 0$ and an outer region $|z| > L_0$, where $\gamma_{\mathrm{r}}^{BT} > 0$ and constant. The effective conductance C^{eff} of the beam tube is given by the reciprocal sum of the effective conductances of the inner ($C_<$) and outer ($C_>$) region,

$$C^{\mathrm{eff}} = \frac{C_< \times C_>}{C_< + C_>}\,. \tag{50}$$

The conductance of the non-recombining inner part is $C_< = C_{\mathrm{BT}}(L/L_0)$ and the effective conductance of the recombining outer part is

$$C_> = C_{\mathrm{BT}}\,\frac{\varepsilon\sqrt{\gamma_{\mathrm{r}}}}{\tanh\left(\varepsilon\sqrt{\gamma_{\mathrm{r}}}\,y_0\right)}, \tag{51}$$

where $y_0 = (L - L_0)/L$. The calculation of the combined conductance yields

$$C^{\mathrm{eff}} = C_{\mathrm{BT}}\,\frac{\varepsilon\sqrt{\gamma_{\mathrm{r}}}}{\varepsilon\sqrt{\gamma_{\mathrm{r}}}\,(1-y_0) + \tanh\left(\varepsilon\sqrt{\gamma_{\mathrm{r}}}\,y_0\right)}\,. \tag{52}$$

The central normalized density $\rho_a(z = 0, \gamma_{\mathrm{r}})$ can be obtained from equation (47)

$$\rho_a(z=0,\gamma_{\mathrm{r}}) = \frac{\sum_i C_i}{\sum_i C_i^{\mathrm{eff}}}\,. \tag{53}$$

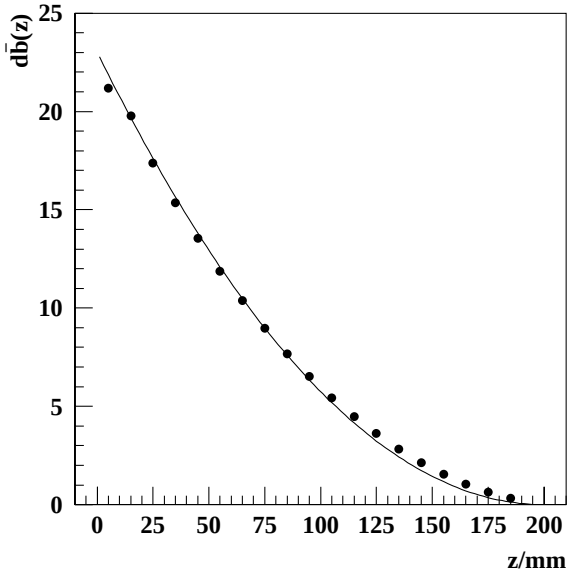

Fig. 6. Average differential collision age of gas in the storage cell center, obtained by a molecular flow simulation (symbols) and by equation (57) (line).

If the conductances of the injection and the sample tube are neglected, one finds

$$\rho_a(z=0,\gamma_{\mathrm{r}}) = 1 - y_0 + \frac{\tanh\left(\sqrt{x}\,y_0\right)}{\sqrt{x}}\,. \tag{54}$$

The first terms of the corresponding Taylor series in γ_{r} are

$$\rho_a(z=0,\gamma_{\mathrm{r}}) = 1 - \frac{1}{3}\,y_0^3\,\varepsilon^2\,\gamma_{\mathrm{r}} \ldots \tag{55}$$

The second term on the right side of equation (55) equals the average number of collisions $\bar{b}_>(L_0)$ (see Eq. (22)) that atoms from the storage cell center carried out in the recombining region ($z > L_0$),

$$\bar{b}_>(L_0) = \frac{1}{3}\,y_0^3\,\varepsilon^2. \tag{56}$$

The average number of collisions $\mathrm{d}\bar{b}(z)$ between z and $z + \mathrm{d}z$ equals the absolute value of the derivative of $\bar{b}_>(L_0)$ with respect to L_0

$$\mathrm{d}\bar{b}(z) = \left(1 - \frac{|z|}{L}\right)^2\,\varepsilon^2\,\frac{\mathrm{d}z}{L}\,. \tag{57}$$

A first order approximation of $\rho_a(0)$ is given by

$$\rho_a(z=0,\gamma_{\mathrm{r}}) = \left(1 + \int_0^L \gamma_{\mathrm{r}}(z)\,\mathrm{d}\bar{b}(z)\right)^{-1}\,. \tag{58}$$

Figure 6 shows a comparison between the second order dependence in z of equation (57) and the simulated differential collision age of the sample gas. The results of the calculation and simulation agree well.

3 The central sampling problem

In the previous section it was shown that the diffusion equation yields a good description of the diffusion process inside a storage cell target. This section will focus on the central sampling problem, as formulated in Section 1. In cases where one can assume a constant recombination (or depolarization) probability γ_r all over the inner surface of a storage cell target and the side tubes, the methods described can be directly used to calculate the atomic fraction inside the storage cell, if the atomic fraction of the gas sample is measured [12,14].

Global uniformity of γ_r is unlikely to occur in a high energy storage ring environment and the measurements at the HERMES target indeed indicate that the storage cell surface is altered by the HERA beam [12,15]. Thus it is required to develop a description for a situation where γ_r is an unknown function of position z along the storage cell. The problem of the determination of γ_r inside the side tubes (sample- and injection tube) will be excluded at this point. There are measurements for the HERMES target which allow one to draw quantitative conclusions about the sample tube properties [12]. In the following it is assumed that γ_r is non-zero only within the beam tube of the storage cell and that the sampled gas represents the properties of the target gas at the storage cell center.

In the steady state $\partial n_a/\partial t = \partial n_a/\partial b = 0$ one may describe the flow of atoms including recombination by equation (28) [19]

$$0 = \frac{\partial n_a}{\partial b} = \tilde{D}\,\frac{\partial^2 n_a}{\partial z^2} - \gamma_\mathrm{r} n_a - k\delta(z), \tag{59}$$

where $k\delta(z)$ represents the injected flux and $\gamma_\mathrm{r} n_a$ the loss in *atomic* density from recombination. γ_r may be an arbitrary positive semidefinite function of position, pressure and temperature. The rate of molecules dissociated by the HERA beam is assumed to be negligible. Hence atoms once recombined do not re-dissociate so

$$\frac{\partial^2 n_a}{\partial z^2} \geq 0 \text{ for } z \neq 0, \tag{60}$$

and hence

$$\left|\frac{\partial n_a}{\partial z}\right| \leq \lim_{z\to 0}\left|\frac{\partial n_a}{\partial z}\right|. \tag{61}$$

It follows that for any function $n_a(z,\gamma_\mathrm{r})$ the following inequality holds

$$\bar{n}_a(\gamma_\mathrm{r}) = \frac{1}{2L}\int_{-L}^{L} n_a(z,\gamma_\mathrm{r})\,\mathrm{d}z \geq n_a(0)\,\frac{z_+ - z_-}{4L}, \tag{62}$$

where z_- and z_+ are defined by

$$\left.\frac{\partial n_a}{\partial z}\right|_{z\to -0} = -\frac{n_a(0)}{z_-}$$
$$\left.\frac{\partial n_a}{\partial z}\right|_{z\to +0} = -\frac{n_a(0)}{z_+}, \tag{63}$$

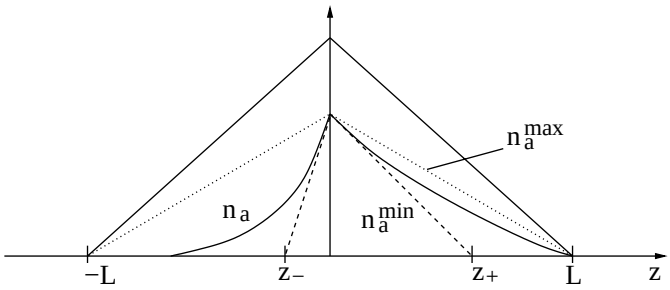

Fig. 7. Illustration of equation (62): the integral of $\int_{-L}^{L} n_a(z,\gamma_\mathrm{r})\,\mathrm{d}z$ is greater than or equal to the area below the dashed lines, and less than or equal to the area below the dotted lines. The solid curve represents the real atomic density $n_a(z,\gamma_\mathrm{r})$ and the triangle of solid straight lines represents the atomic density without recombination $n_a(z,\gamma_\mathrm{r}=0)$.

as illustrated in Figure 7. The injected flux of the ABS $\dot{n}^\mathrm{inj}$ reaches the center of the storage cell *ballistically* and, in case of the HERMES storage cell, starts to diffuse into four different tubes ($\dot{n}^\mathrm{ET} = \dot{n}^\mathrm{ST}$)

$$\dot{n}^\mathrm{inj} = \dot{n}^\mathrm{IT} + \dot{n}^\mathrm{ST} + \dot{n}^\mathrm{BT}_+ + \dot{n}^\mathrm{BT}_-, \tag{64}$$

where $\dot{n}^\mathrm{BT}_\pm$ are the fluxes into the right and left side of the beam tube, respectively. With equation (1) this can be written as

$$\dot{n}^\mathrm{inj} = \dot{n}^\mathrm{IT} + \dot{n}^\mathrm{ST} + D^\mathrm{BT} S^\mathrm{BT}\left(\left.\frac{\partial n_a}{\partial z}\right|_{z\to -0} - \left.\frac{\partial n_a}{\partial z}\right|_{z\to +0}\right), \tag{65}$$

and therefore with equation (63)

$$\dot{n}^\mathrm{inj} = \dot{n}^\mathrm{IT} + \dot{n}^\mathrm{ST} + D^\mathrm{BT} S^\mathrm{BT}\, n_a(0)\left(\frac{1}{z_+} - \frac{1}{z_-}\right). \tag{66}$$

The central atomic density $n_a(z=0,\gamma_\mathrm{r})$ can be computed using equation (66)

$$n_a(0,\gamma_\mathrm{r}) = \frac{\dot{n}^\mathrm{inj}}{C^\mathrm{IT} + C^\mathrm{ST} + D^\mathrm{BT} S^\mathrm{BT}\,(1/z_+ - 1/z_-)}, \tag{67}$$

where $\dot{n}^\mathrm{IT} = n_a(0)\,C^\mathrm{IT}$ and $\dot{n}^\mathrm{ST} = n_a(0)\,C^\mathrm{ST}$ have been used.

It is readily shown that for a given $n_a(0,\gamma_\mathrm{r})$, $\bar{n}_a(\gamma_\mathrm{r})$ is minimum in the symmetric case where $z_+ = z_-$. The minimum possible average atomic density in the storage cell, consistent with an observed density $n(0,\gamma_\mathrm{r})$ in the center, is

$$\bar{n}_a(\gamma_\mathrm{r}) \geq \frac{1}{2} n_a(0,\gamma_\mathrm{r})\frac{z_0}{L}, \tag{68}$$

where $z_0 = z_+ = -z_-$ was used. z_0/L can be expressed using equation (67)

$$\frac{z_0}{L} = \frac{2\,C^\mathrm{BT}}{\dot{n}^\mathrm{inj}/n_a(0) - C^\mathrm{IT} - C^\mathrm{ST}}, \tag{69}$$

where $C^{\mathrm{BT}} L^{\mathrm{BT}} = D^{\mathrm{BT}} S^{\mathrm{BT}}$ was used. The ratio η of the conductances of the side tubes to the beam tube is defined by

$$\eta = \frac{C^{\mathrm{IT}} + C^{\mathrm{ST}}}{2\,C^{\mathrm{BT}}}\,. \tag{70}$$

Equation (68) then gives

$$\bar{n}_a(\gamma_{\mathrm{r}}) \geq \frac{1}{2}\,\frac{n_a(0,\gamma_{\mathrm{r}})}{\dot{n}^{\mathrm{inj}}/[n_a(0)\,2C^{\mathrm{BT}}] - \eta}\,. \tag{71}$$

The survival probabilities can be calculated by equation (37)

$$\bar{\rho}_a = \frac{\bar{n}_a(\gamma_{\mathrm{r}})}{\bar{n}_a(\gamma_{\mathrm{r}}=0)} = \frac{\bar{n}_a(\gamma_{\mathrm{r}})}{\dot{n}^{\mathrm{inj}}}\,2\,C^{\mathrm{tot}}, \tag{72}$$

and

$$\rho_a(0,\gamma_{\mathrm{r}}) = \frac{n_a(0,\gamma_{\mathrm{r}})}{n_a(0,\gamma_{\mathrm{r}}=0)} = \frac{n_a(0,\gamma_{\mathrm{r}})}{\dot{n}^{\mathrm{inj}}}\,C^{\mathrm{tot}}, \tag{73}$$

where $C^{\mathrm{tot}} = 2\,C^{\mathrm{BT}} + C^{\mathrm{IT}} + C^{\mathrm{ST}} = 2\,C^{\mathrm{BT}}\,(1+\eta)$. The factor 2 in equation (72) originates from the averaging of the triangular density profile. Multiplication of equation (71) with $2\,C^{\mathrm{tot}}/\dot{n}^{\mathrm{inj}}$ yields

$$\bar{\rho}_a \geq \frac{\rho_a^2(0)}{1+\eta\,(1-\rho_a(0))}\,. \tag{74}$$

This inequality provides the following interpretation: if one is able to determine the relative atomic density in the storage cell center, the *average* relative atomic density all over the storage cell, $\bar{\rho}_a$, can not be less than the value given by equation (74), independent of the functional form of γ_{r}. It should be stressed, that this lower limit can only be reached in the extreme case, where γ_{r} is a step function

$$\begin{aligned} \gamma_{\mathrm{r}} &= 0 \quad \text{for } |z| \leq z_0 \\ \gamma_{\mathrm{r}} &= 1 \quad \text{for } |z| > z_0. \end{aligned} \tag{75}$$

The condition for the maximum average atomic density is defined by the dotted line in Figure 7,

$$\int_{-L}^{L} n_a(z,\gamma_{\mathrm{r}})\,\mathrm{d}z \leq n_a(0,\gamma_{\mathrm{r}})L, \tag{76}$$

and hence

$$\bar{n}_a(\gamma_{\mathrm{r}}) = \frac{1}{2\,L}\int_{-L}^{L} n_a(z,\gamma_{\mathrm{r}})\,\mathrm{d}z \leq \frac{n_a(0,\gamma_{\mathrm{r}})}{2}\,. \tag{77}$$

Since $n_a(0,\gamma_{\mathrm{r}}=0) = 2\bar{n}_a(\gamma_{\mathrm{r}}=0)$ holds for a triangular distribution, the normalization yields

$$\bar{\rho}_a(\gamma_{\mathrm{r}}) = \frac{\bar{n}_a(\gamma_{\mathrm{r}})}{\bar{n}_a(\gamma_{\mathrm{r}}=0)} \leq \frac{n_a(0,\gamma_{\mathrm{r}})}{2\bar{n}_a(\gamma_{\mathrm{r}}=0)} = \rho_a(0), \tag{78}$$

so that

$$\rho_a(0,\gamma_{\mathrm{r}}) \geq \bar{\rho}_a(\gamma_{\mathrm{r}}) \geq \frac{\rho_a^2(0,\gamma_{\mathrm{r}})}{1+\eta\,(1-\rho_a(0,\gamma_{\mathrm{r}}))}\,. \tag{79}$$

For HERMES, the properties of the gas diffusing out the sample tube are not identical to the properties of the gas in the storage cell center, because in the sample tube recombination or depolarization may occur as well. Accordingly, the normalized density of atoms in the sampled gas $\rho_a^{\mathrm{s}}(\gamma_{\mathrm{r}})$ is always less or equal to $\rho_a(0,\gamma_{\mathrm{r}})$. Hence the upper limit of $\bar{\rho}_a(\gamma_{\mathrm{r}})$ for a given measured value ρ_a^{s} is a weaker limit than the lower limit and holds only in case of vanishing recombination in the sample tube.

4 The atomic fraction

We define the atomic fraction α in any region of a hydrogen or deuterium gas target as the ratio of the density of nuclei in atoms to the total density of nuclei (in atoms and molecules) in that region.

$$\alpha = \frac{n_a}{n_a + 2\,n_m} = \frac{p_a}{p_a + 2\,p_m}, \tag{80}$$

where n_a and n_m are the densities of atoms and molecules and p_a and p_m are the partial pressures of atoms and molecules, respectively. The continuity equation (4) is then written in the following way

$$\dot{n}_a + \boldsymbol{\nabla} \boldsymbol{j}_a + 2(\dot{n}_m + \boldsymbol{\nabla} \boldsymbol{j}_m) = 0. \tag{81}$$

In case of continuous flow ($\dot{n}_a = \dot{n}_m = 0$) this equation leads to

$$\frac{\mathrm{d}}{\mathrm{d}z}(\Phi_a + 2\Phi_m) = 0, \tag{82}$$

so that

$$\Phi_a + 2\Phi_m = -C_a L\frac{\mathrm{d}p_a}{\mathrm{d}z} - 2\,C_m L\frac{\mathrm{d}p_m}{\mathrm{d}z} = \Phi_{\mathrm{tot}} = const, \tag{83}$$

where Φ_a and Φ_m are the net (particle) fluxes of atoms and molecules along the cell, respectively. Φ_{tot}, the total flux along the cell, is proportional to the output flux of the ABS and is therefore independent of γ_{r} and z. If one can assume that the hot molecules produced in the recombination process, cool down to the temperature of the storage cell within a few wall collisions, atoms and molecules are at the same temperature. Since the molecules are twice as heavy their thermal velocity and conductance C_m are given by

$$C_m = \frac{1}{\sqrt{2}}\,C_a, \tag{84}$$

so that

$$\frac{\mathrm{d}}{\mathrm{d}z}(p_a + \sqrt{2}\,p_m) = const. \tag{85}$$

Integration of the left side yields the integrand, the right side a linear function in z. One may express the result including the boundary condition of vanishing pressures at the end of the tube by

$$p_a + \sqrt{2}\, p_m = p_0\, \frac{L - |z|}{L}\,. \tag{86}$$

The constant p_0 is independent of γ_r. It depends only on the intensity of the injected atomic beam and the overall cell properties such as geometry and wall temperature, all of which are assumed to be constant. In the absence of recombination p_0 is equal to the magnitude of the cell gas pressure at $z = 0$. It follows from equation (86) that the sum $p_a + \sqrt{2}\, p_m$ is of triangular shape for any γ_r, including the non-uniform case described in the next section. The total gas pressure $p_a + p_m$ and the total nucleon density, proportional to $p_a + 2\, p_m$, both depend on γ_r. Furthermore, equation (86) implies a non-linear relationship between α and p_a.

In the following, rather than using p_a, $\sqrt{2}\, p_m$ and $p_a + 2\, p_m$, it is useful to normalize these quantities to $p_a + \sqrt{2}\, p_m$ by defining the normalized variables ρ_a and ρ_m and the normalized total density ρ_t by

$$\rho_a(z) = \frac{p_a}{p_a + \sqrt{2}\, p_m}$$

$$\rho_m(z) = \frac{\sqrt{2}\, p_m}{p_a + \sqrt{2}\, p_m} \tag{87}$$

$$\rho_\mathrm{t}(z) = \frac{p_a + 2\, p_m}{p_a + \sqrt{2}\, p_m}, \tag{88}$$

where

$$\rho_a + \rho_m = 1. \tag{89}$$

The variable ρ_a is of particular interest here because it is equivalent to the survival probability, defined by equation (19). The normalized total density ρ_t may be expressed in terms of ρ_a

$$\rho_\mathrm{t} = \rho_a + \sqrt{2}\, \rho_m = \sqrt{2} - (\sqrt{2} - 1)\rho_a, \tag{90}$$

and depends on the strength of the recombination process. The atomic fraction α is given by

$$\alpha(z, \gamma_\mathrm{r}) = \frac{\rho_a}{\rho_t} = \frac{\rho_a}{\sqrt{2} - (\sqrt{2} - 1)\rho_a}, \tag{91}$$

and the total normalized target density ρ_t is

$$\rho_\mathrm{t} = \frac{\sqrt{2}}{1 + (\sqrt{2} - 1)\alpha}\,. \tag{92}$$

The fact that ρ_t depends on the atomic fraction may in principle be used for the determination of α, but the achievable precision in case of the HERMES target is insufficient [15]. The relations between ρ_a, ρ_m, ρ_t and α are shown in Figure 8. Making use of the fact that ρ_a is equivalent to the survival probability, one can determine

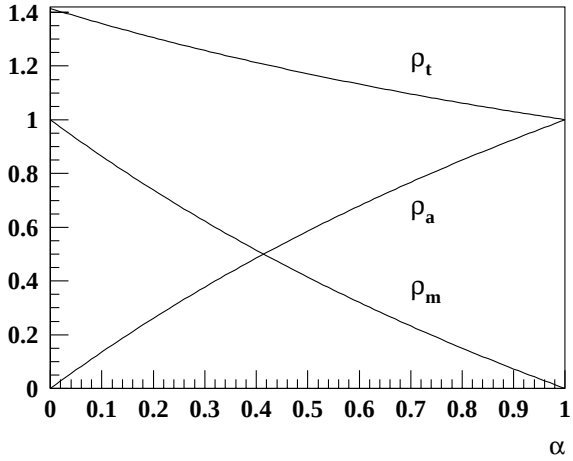

Fig. 8. Normalized densities ρ_a and ρ_t in the storage cell plotted *vs.* the atomic fraction α. The variable $\rho_m = 1 - \rho_a$ is also shown.

limits for the (density weighted) average value of α from a known value $\rho_a(0)$ by applying equation (79)

$$\alpha \le \frac{\sqrt{2}\, \rho_a(0)}{1 + (\sqrt{2} - 1)\, \rho_a(0)}$$

$$\alpha \ge \frac{\rho_a(0)^2}{\sqrt{2}\, [1 + \eta\, (1 - \rho_a(0))] - (\sqrt{2} - 1)\, \rho_a(0)^2}. \tag{93}$$

The relative systematic uncertainty is calculated by

$$\frac{\Delta\alpha}{\alpha} = \frac{\alpha_\mathrm{max} - \alpha_\mathrm{min}}{\alpha_\mathrm{max} + \alpha_\mathrm{min}}, \tag{94}$$

and shown *vs.* $\rho_a(0)$ in the right graph of Figure 9. Even though the uncertainty becomes large if α deviates significantly from unity, it is below about $1 - \alpha$ and hence small for high values of α ($\alpha > 0.95$), typically measured at the HERMES target. This statement is especially true if one takes into account that the limiting cases are only reached in the unrealistic situation of extremely non-uniform surfaces.

5 Conclusion and summary

It has been shown that the wall CAD of rarefied gases diffusing in long tubes can be calculated analytically from the diffusion equation with high precision. In cases of low recombination, the knowledge of the average collision age has been shown to be sufficient to calculate the amount of recombination. A measurement on a gas sample taken from the center of the storage cell can be used to derive the average atomic fraction within the storage cell, if recombination is assumed to be uniform. In the case of an arbitrary non-uniform surface, the properties of the gas sample were used to obtain limits for the average atomic fraction. The relative systematic uncertainty in this case is roughly equal to the measured fraction of molecules and hence is small in a target with low recombination, *e.g.*

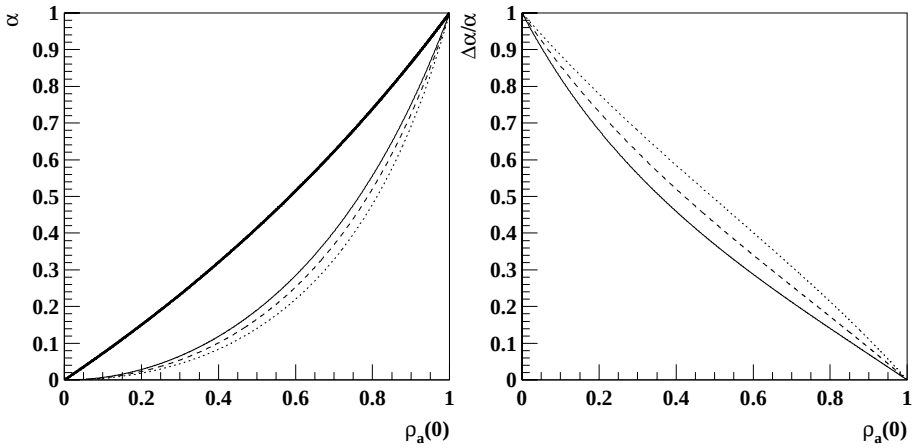

Fig. 9. Left: Limits of the possible values of the atomic fraction α in a storage cell as a function of the measured density of atoms at the cell center $\rho_a(0)$. The three thin curves represent the lower limits of α for different injection tube geometries. The solid thin curve represents a scenario with $\eta = 0$, *i.e.* for the hypothetic case of no side tubes, the dashed curve is calculated for the former HERMES storage cell (see Fig. 1) and the dotted curve for the actual storage cell which has a reduced beam tube cross-section [12]. The thick solid curve is the (common) upper limit. Right: Relative systematic uncertainty for the same cases.

at the working point of the HERMES target. A similar formalism can be applied to spin relaxation in wall collisions [12].

This work was supported by the German Bundesministerium für Bildung, Wissenschaft, Forschung und Technologie (BMBF 056MU22I(1) and 057ER12P(2)); the UK Particle Physics and Astronomy Research Council; the US Department of Energy and the National Science Foundation; the Dutch Foundation for Fundamenteel Onderzoek der Materie (FOM) and the Italian Instituto Nazionale di Fisica Nucleare (INFN).

References

1. H.O. Meyer, J.T. Balewski, M. Dzemidzic, J. Doskow, R.E. Pollock, B. von Przewoski, T. Rinckel, F. Sperisen, P. Thoerngren-Engblom, M. Wolanski, W. Haeberli, B. Lorentz, F. Rathmann, B. Schwartz, T. Wise, W.W. Daehnick, R.W. Flammang, Swapan K. Saha, D.J. Tedeschi, P.V. Pancella, Phys. Rev. Lett. **81**, 3096 (1998).
2. D. Albers, J. Bisplinghoff, R. Bollmann, K. Büßer, P. Cloth, R. Daniel, O. Dichl, F. Dohrmann, H.P. Engelhardt, J. Ernst, P.D. Eversheim, M. Gasthuber, R. Gebel, J. Greiff, A. Groß, R. Groß-Hardt, S. Heider, A. Heine, F. Hinterberger, M. Igelbrink, R. Jahn, M. Jeske, U. Lahr, R. Langkau, J. Lindlein, R. Meier, R. Mashuw, T. Mayer-Kuckuk, F. Mosel, M. Müller, M. Münstermann, D. Prasuhn, H. Rohdjeß, D. Rosendaal, U. Roß, P. von Rossen, H. Scheid, N. Schirm, M. Schulz-Rojahn, F. Schwandt, V. Schwarz, W. Scobel, G. Sterzenbach, H.J. Trelle, A. Wellinghausen, W. Wiedmann, K. Woller, R. Ziegler, Phys. Lett. **78**, 1652 (1997).
3. R.G. Milner, Nucl. Phys. A **622**, 16c (1997).
4. HERMES-Proposal, HERMES Collaboration 1990; DESY-PRC-90/91.
5. HERMES Technical Design Report, HERMES Coll. 1993; DESY-PRC 93/06.
6. T. Wise, A.D. Roberts, W. Haeberli, Nucl. Instr. Meth. A **336**, 410 (1993).
7. R. Gilman, R.J. Holt, E.R. Kinney, R.S. Kowalczyk, J. Napolitano, A.W. Nikitin, D.M. Nikolenko, S.G. Popov, D.H. Potterveld, I.A. Rachek, D.K. Toporkov, E.P. Tsentalovich, B.B. Wojtsekhowski, L. Young, Nucl. Instr. Meth. A **327**, 277 (1993).
8. M.A. Ross, W.K. Pitts, W. Haeberli, H.O. Meyer, S.F. Pate, R.E. Pollock, B. von Przewoski, T. Rinckel, J. Sowinski, F. Sperisen, P.V. Pancella, Nucl. Instr. Meth. A **326**, 424 (1993).
9. J. Stewart, G. Court, W. Haeberli, J. Morton, H. Tallini, T. Wise, K. Zapfe-Düren, in: *6th Int. Workshop on Pol. Beams and Pol. Gas Targets*, pp. 408-412, Cologne, 1995, (World Scientific, 1996).
10. W. Haeberli, Ann. Rev. Nucl. Sci. **17**, 373 (1967).
11. F. Stock, K. Rith, H.G. Gaul, B. Lorentz, H. Mairon, B. Povh, E. Steffens, D. Toporkov, K. Zapfe, F. Rathmann, D. Fick, W. Korsch, G. Graw, K. Reinmüller, P. Schiemenz, W. Haeberli, Nucl. Instr. Meth. A **343**, 334 (1994).
12. C. Baumgarten, Ph.D. thesis (english), Ludwigs-Maximilians-Universität München (2000); `www.ub.uni-muenchen.de/elektronische_dissertationen/physik/Baumgarten_Christian.pdf`.
13. B. Braun, Ph.D. thesis, Ludwigs-Maximilians-Universität München (1995); german original: `hermes.desy.de/notes/pub/95-LIB/braun.95.047.thesis.ps.gz`; english translation: `hermes.desy.de/notes/pub/95-LIB/braun.95.047e.thesis.ps.gz`.
14. C. Baumgarten, Diploma thesis, Universität Hamburg (1996); `hermes.desy.de/notes/pub/96-LIB/baumgarten.96.068.ps.gz`.
15. H. Kolster, Ph.D. thesis (english), Ludwigs-Maximilians-Universität München (1998); `hermes.desy.de/notes/pub/98-LIB/kolster.98.009.ps.gz`.

16. M. Henoch, Diploma thesis, Universität Münster (1998); `hermes.desy.de/notes/pub/99-LIB/henoch.99.003.thesis.ps.gz`.
17. H.-G. Gaul, E. Steffens, Nucl. Instr. Meth. A **316**, 297 (1992).
18. C. Baumgarten, B. Braun, G. Court, G. Ciullo, P. Ferretti, A. Golendukhin, G. Graw, W. Haeberli, M. Henoch, R. Hertenberger, N. Koch, H. Kolster, P. Lenisa, A. Nass, S.P. Pod'yachev, D. Reggiani, K. Rith, M.C. Simani, E. Steffens, J. Stewart, T. Wise, accepted for publication in Nucl. Instr. Meth. A.
19. J.T.M. Walraven, F. Silvera, Rev. Sci. Instrum. **53**, 1167 (1982).
20. M. Knudsen, Ann. Physik **28**, 75, 999 (1909).
21. M. v. Smoluchowski, Ann. Physik **33**, 1559 (1910).
22. W. Gaede, Ann. Physik **41**, 289 (1913).
23. A.E. Fick, Ann. Physik **94**, 59 (1855).
24. P. Clausing, Ann. Phys. **12**, 961 (1932); a translation to english can be found in: J. Vac. Sci. Techn. **8**, 636 (1971).
25. W.G. Pollard, R.D. Present, Phys. Rev. **73**, 762 (1948).
26. L.M. Lund, A.S. Berman, J. Appl. Phys. **37**, 2489 (1966).
27. J.C. Helmer, J. Vac. Sci. Techn. **4**, 360 (1967).
28. C.A. Flory, L.S. Cutler, J. Appl. Phys. **73**, 1561 (1993).
29. The molecular flow simulation was done by two independent trajectory tracing programs by the HERMES target group. Both simulations are based on the assumption of a $\cos\theta$-distribution of the desorption angle relative to the surface normal. More details can be found in [12–16].
30. A. Sommerfeld, Partielle Differentialgleichungen der Physik, Geest & Portig, Leibzig 1947; Nachdruck von Harri Deutsch, Thun, 1978.
31. M. Abramowitz, I.A. Stegun, Pocketbook of Math. Func., orig. publ. by the Nat. Bureau of Standards 1964 (Harri Deutsch, Thun, 1984).